ARTICLE IN PRESS

Available online at www.sciencedirect.com

SCIENCE DIRECT®

ELSEVIER

New Astronomy Reviews xxx (2004) xxx–xxx

New Astronomy Reviews

www.elsevier.com/locate/newastrev

Deep radio continuum studies with the SKA: evolution of radio AGN populations

C.A. Jackson

CSIRO Australia Telescope National Facility, Sydney, Australia

Abstract

Radio emission is insensitive to dust obscuration, and the breadth of the radio luminosity function ensures that sources are detected over a wide range of redshifts at all radio flux densities. As a result, radio continuum observations are an efficient and unbiased probe of both nuclear (AGN) and star-forming activity over all cosmic epochs.

The SKA's ultra-deep radio continuum surveys will provide the answers to at least three key astrophysical questions: (i) the star-formation history of the Universe, (ii) the evolution of the low-power end of the radio galaxy luminosity function and (iii) the relationship between the radio-loud AGN, star-formation and radio-quiet AGN phenomena.

In this paper, we discuss the AGN science that will be enabled by the deep radio continuum studies using the SKA. It is important to recognise that the sub-μJy SKA sky will be dominated by populations other than 'radio-loud' AGN. In this way the SKA will not only provide an unbiased tracer of the star-formation history of the Universe but also be able to study the populations of sources we currently describe as 'radio-quiet'. To illustrate this point we present simulations of the extragalactic radio sky based from models of the evolution of the radio luminosity function. From these simulations we predict typical source distributions and estimate the natural confusion limit to ultra-faint flux density limits relevant to the science and design goals of the SKA.

1. Introduction

As a consequence of the broad radio luminosity function (RLF) which spans many decades in radio power, radio continuum observations at all flux density limits detect extragalactic sources across a wide redshift range. Current large-area radio surveys, e.g., the NRAO VLA Sky Survey (NVSS, Condon et al., 1998), Faint Images of the Radio Sky at twenty cm (FIRST, White et al., 1997) and the Sydney University Molonglo Sky Survey (SUMSS, Bock et al., 1999), cover thousands of square degrees of sky to mJy-flux density limits. These surveys are the deepest practicable over large areas of sky given the large amounts of observing time involved. Surveys to increasingly fainter flux density limits cover far

E-mail address: carole.jackson@csiro.au.

1387-6473/$ - see front matter
doi:10.1016/j.newar.2004.09.023

smaller areas, e.g. the Australia Telescope ESO Slice Project (ATESP, Prandoni et al., 2001) covers 26 square degrees at 1.4 GHz to $S_{1.4\ \mathrm{GHz}} = 0.4$ mJy (5σ rms) whereas the VLA observations of the Hubble Deep Field (north) area covers just 0.35 square degrees (Richards, 2000) to $S_{1.4\ \mathrm{GHz}} = 0.04$ mJy (5σ rms).

The SKA, with its significantly larger collecting areas, will be capable of large-area sub-μJy surveys as well as deep nano-Jy small-area surveys. The challenge is to determine what the sky might look like at these faint limits. Firstly it is obvious that the SKA will be able to compile a complete census of AGN throughout the Universe, mapping their evolution and reveal the relationship between the various populations. In turn this will allow us to unravel the underlying physics of the AGN lifecycle (Jarvis and Rawlings, 2004; Falcke et al., 2004). The key AGN questions are:

- When do the first AGN form? What is their role in the epoch of reionization?
- What drives the evolution of AGN? Is it in-fall of material via mergers, internally-changing accretion rates?
- That is the typical lifecycle of an AGN? Is it the same galaxies re-activating?
- How many populations of AGN are there?
- Is there a continuum of AGN activity, from the super-Eddington accretors to normal galaxies (and perhaps to even lower-power/low mass objects)? Are there objects with BH's of a few hundred solar masses?
- What is the interplay (if any) between AGN activity and star formation?

In this contribution, we concentrate on how SKA deep continuum surveys will revolutionise our study of the AGN phenomenon in light of our current knowledge.

2. Radio-loud AGN, continuum surveys and the RLF

Bright continuum radio surveys reveal sources which are powered by non-thermal (synchrotron) radio emission from AGN embedded within individual galaxies span a huge range in luminosities. AGN activity is detected across a huge radio luminosity range from between 10^{22} and 10^{28} W Hz^{-1} at 1.4 GHz.

At low radio powers we find classes of objects more usually termed radio-quiet' AGN: These include Seyfert galaxies and QSOs. Because of the huge range of observed luminosities, it can be argued that a continuum of nuclear radio activity exists – such that all galaxies may harbour a central MBH and it is only periodical triggering of activity which gives rise to radio jets and lobes

Radio sources are classified by types, e.g., normal galaxies, Seyferts, FRI or FRII radio galaxies or quasars, based on their luminosity, radio morphology, radio spectral index, variability, optical counterpart and IR, optical and X-ray spectral features.

The existence of a continuum of radio activity is clear, with the various source populations overlapping at all but the highest radio luminosities. This is clearly seen in recent, accurate determinations of the local radio luminosity function (LRLF, Condon et al., 2002; Sadler et al., 2002) for moderate power radio sources (10^{22}–10^{24} W Hz^{-1}) derived from comprehensive galaxy redshift surveys (UGC, 2dFGRS, SDSS) matched to large-area radio surveys (NVSS, FIRST, SUMSS). At lower radio luminosities, the LRLF can only be compiled by observing individual objects for long integration times. At the high luminosity end the space density of objects is small at all epochs, so that all that can be determined is the sparsely-sampled (evolving) RLF from large-area samples (e.g., Wall et al., 2001). Moreover the high luminosity end of the LRLF can *only* be derived from evolutionary fits to the source count, as it cannot be directly determined due to the very low local space density of these objects.

In terms of source types, powerful extragalactic radio sources are a mixture of radio-loud galaxies, quasars and BL Lac objects – all members of the Active Galactic Nuclei (AGN) class of objects. At the zeroth level, radio galaxies can be classified as either Fanaroff-Riley class I or II (FRI or FRII): these are distinguished by the distribution of bright knots of radio emission and collimation features (Fanaroff and Riley, 1972). In general, FRIs are of lower radio power than FRIIs, although there is considerable overlap in the radio luminosity function of the two classes. The current paradigm for radio-loud AGN attributes FRI and FRII radio galaxies as the 'parent' populations of the great majority of the observed powerful AGN (e.g., Urry and Padovani, 1995), such that quasars, blazars and BL Lac objects are manifestations of FRI and FRII radio galaxies aligned close to our line of sight, with their core radio emission Doppler-beamed (Jackson and Wall, 1999 and references therein).

Typically, FRI and FRII radio sources have linear dimensions of the order of between one and a few hundred kilo-parsecs. Their radio structure shows a pair of oppositely directed radio lobes which are sometimes joined to the radio core via a pair of collimated, knotty jets of bright radio emission. The radio emission from the lobes of FRI and FRII radio galaxies is usually optically thin with a radio spectral index around −0.7, although these sources may also have a self-absorbed flat-spectrum core. Compact radio quasars, and radio galaxy cores, typically have angular dimensions much less than an arc-second, and due to self-absorption have flat radio spectra. The compact radio sources (quasars and blazars) are often variable across a wide waveband (radio-to-UV) and their host galaxies may show broad optical/UV emission line spectra.

The study of the evolution of the most powerful radio-loud AGN is based on the RLF. It is well established that powerful evolution is required, for both these objects, and radio-quiet QSOs: The form of this evolution whether luminosity evolution (Boyle et al., 1998) or luminosity-density evolution (Dunlop and Peacock, 1990) is not yet determined, but pure luminosity evolution infers source lifetimes which are unphysical (Haehnelt and Rees, 1993). Observations at SKA sensitivities are required to detect low power radio sources at high redshift; this will determine whether all radio-loud AGN co-evolved or if we are seeing multiple populations undergoing bursts of AGN activity.

Classification of individual radio sources is often hampered by the difficulty of optical/IR/UV follow-up: if the optical host is identifiable it can still be too faint for 8-m class spectroscopy. Fortunately cross-waveband detection may not be a requirement for the SKA as the distinction between AGN and/or star-formation activity is best made via VLBI-scale imaging of μJy sources.

2.1. Radio sources and the SKA

Significant progress has been made in understanding the general radio AGN phenomenon from both

(i) wide and shallow sky surveys, cataloguing up to 100 sources per square degree to about 1 mJy (e.g., FIRST), and
(ii) small and deep pencil beam surveys ($\ll$1 degree areas), to very faint flux densities e.g., the Hubble Deep Field North and other fields (Fomalont et al., 2002) and the Hubble Deep Field South (Norris et al., 2001).

The primary gain of the SKA will be its ability to reach deep sensitivity limits and probe the enormous span of AGN radio powers across a wide redshift range. This will remove the luminosity-redshift ($P-z$) degeneracy which plagues flux density limited samples of today: at significant redshifts ($z > 1$) only the highest-power sources are detected (Blundell et al., 1999).

Multi-wavelength (optical/UV) imaging and spectroscopy of sources in the wide and shallow surveys have revealed that the vast majority of radio sources stronger than a few mJy at 1.4 GHz are powerful radio galaxies or quasars. Moreover, due to the steepness of the high radio power RLF, coupled with strong cosmic evolution between $z = 1$ and 5, the *entire* population of high power radio AGN is sampled above a few mJy: below this flux density limit the nature of the radio source population changes dramatically. Small, deep pencil beam surveys reveal that below about 1 mJy at 1.4 GHz, the differential radio source count flattens: both the star forming galaxy population and galaxies with low power AGN contribute. The contribution from, and physical properties of the star forming galaxies is discussed in van der Hulst et al. (2004).

3. The SKA extragalactic continuum sky

The SKA will offer significant improvement in sensitivity so that it will be possible to detect radio emission as weak as 10 nJy within ∼1000 h integration time. In this way, the SKA will probe a huge part of the very broad RLF at all epochs and the misnomers of radio-loud–radio-quiet may be buried forever.

High resolution, multi-wavelength observations will be critical to distinguish those extragalactic radio sources with AGN emission processes. Whilst nothing is known about the radio source count below about 30 μJy, some estimates can be made by extrapolating the RLF to low luminosities (10^{18} W Hz^{-1}) and adopting evolution models which match the observed evolution of the more powerful sources.

3.1. Simulating the radio source sky

Simulations of the extragalactic radio sky, based on number density predictions from models of the evolution of the radio luminosity function allow us to predict typical source distributions and natural confusion limit to projected SKA flux density limits. We show some examples here for a lambda-dominated WMAP cosmology ($\Omega_m = 0.23$, $\Omega_\Lambda = 0.73$ and $H_0 = 71$ km s^{-1} Mpc^{-1}).

We start by assuming that the radio sky comprises three populations of sources, namely FRI, FRII and star-forming galaxies, and the LRLF and evolution for each can be determined: For the star-forming galaxy population we adopt the local radio luminosity function from the 2 dFGRS-NVSS galaxy sample at 1.4 GHz (Sadler et al., 2002). We adopt parameterised number-density luminosity evolution for the star-forming population as determined from the HDF-N and SSA13 fields (Haarsma et al., 2000).

The local radio luminosity functions and evolution for the FRI and FRII radio galaxies are derived using the methodology of Jackson and Wall (1999). In summary, we fit exponential luminosity-dependent density evolution (LDDE) to the observed source count at 151 MHz. We find a best-

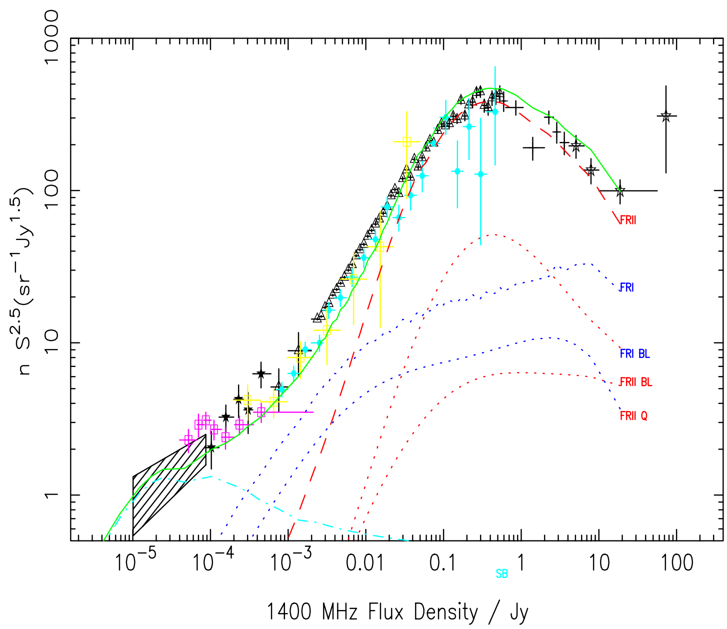

Fig. 1. Normalised observed and model differential source counts at 1.4 GHz. The model count comprises three populations: FRII radio galaxies (dashed line), FRI radio galaxies (dotted) and star-forming galaxies (dot-dash). Data points are from: ☆ Bridle et al. (1972), + Fomalont et al. (1974), △ White et al. (1997), ☆ Mitchell and Condon (1985), ○ Prandoni et al. (2000); □ Gruppioni et al. (1997) and ∗ Richards (2000). The polygon is the count estimate from the $P(D)$ (background-deflection) analysis of Wall and Cooke (1975).

fit to the observed 151 MHz source count for LDDE of the FRII population, $\phi_z = F(P, z) \cdot \phi_0$, where ϕ_0 is the LRLF. For the function $F(P, z)$ we fit $M_{\max} = 15.70$, $z_c = 7.425$, $P_1 = 25.94$ $P_2 = 27.94$ for the FRII population, coupled with mild ($M = -3.06$) density evolution of the FRI population.

From the three evolving RLFs we can produce simulated sky regions at a range of SKA frequencies: at 1.4 GHz we use the evolutionary fit at 151 MHz plus 'beaming factors' to account for the quasar and BL Lac populations (Fig. 1). For a single sky simulation we randomly position each source within a specified sky area. Each source is then randomly oriented, both on and into the plane. FRI and FRII radio galaxies are randomly assigned a total intrinsic size (lobe-to-lobe) between 50 and 800 kpc (as observed for the powerful 3CR sources, Laing et al., 1983), assuming no source size evolution with redshift. FRIs and FRIIs are modeled as double-lobe structures, with each lobe being half the intrinsic total size adjusted for source orientation and redshift, i.e., foreshortened and flattened. Doppler-beamed versions of the FRI and FRIIs are set to be point sources. Star-forming galaxies are modelled as a circular

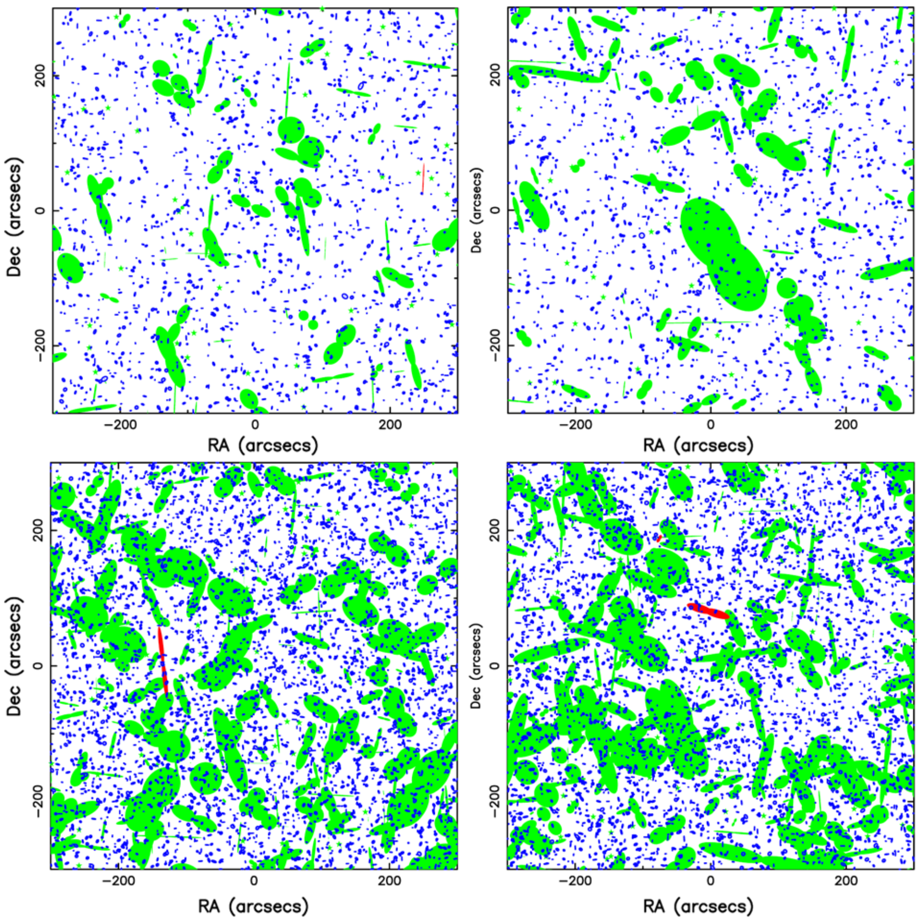

Fig. 2. Simulated sky images at 1.4 GHz, showing a 10′ square region for flux density limits of 1 μJy (upper) and 100 nJy (lower). The difference between the pair of images at the same flux density illustrates cosmic variance, with nearby large-lobed sources dominating the right-hand plots. There are five populations of sources shown: FRI galaxies (light, double-lobed), FRII galaxies (dark, double-lobed), starforming galaxies (dark, single disk), beamed FRIIs (dark, star), and FRIs (light, star).

Table 1
Predicted source surface densities at 1.4 GHz

Population	Flux density limit					
	10 μJy		1 μJy		100 nJy	
	$N(\deg^2)$	Cover fraction	$N(\deg^2)$	Cover fraction	$N(\deg^2)$	Cover fraction
FRI	1207	4×10^{-2}	4028	0.136	10,162	0.340
FRII	55	3×10^{-3}	56	3×10^{-3}	56	3×10^{-3}
Star-forming	7361	2×10^{-3}	52,798	2×10^{-2}	135,806	0.05
Total	8623	5×10^{-2}	56,822	0.162	146,024	0.394
Minimum resolution (″)	0″.86		0″.17		0″.07	
% of sources overlapped (line-of-sight)	10%		25%		60%	

Table 2
Predicted source distribution per square degree at 1.4 GHz

Redshift	Flux density limit								
	10 μJy			1 μJy			100 nJy		
	N(FRI)	N(FRII)	N(SF)	N(FRI)	N(FRII)	N(SF)	N(FRI)	N(FRII)	N(SF)
$z < 1$	718	2	2556	1636	2	9759	2570	2	14,238
$z < 3$	1145	21	6740	3202	21	42,865	6551	21	100,453
$z < 5$	1190	42	7361	3644	42	52,798	7955	42	135,806
$z > 5$	17	13	0	384	13	0	2207	13	0

disks with a randomly assigned intrinsic disk diameter between 10 and 100 kpc: these sizes are generous given the increasing evidence that spiral disks at high redshift are significantly smaller (e.g., Giallongo et al., 2000). These disks are oriented randomly on the plane of the sky. Examples are shown here (Fig. 2), a wider range of simulated sky images, at 151 MHz, 325 MHz and 1.4 GHz, are available at http://www.atnf.csiro.au/~cjackson/lowfreq_sky.

We can predict the number of sources per square degree and the fraction of sky covered by each population at 1.4 GHz as shown in Table 1. We estimate the minimum resolution which would give an average inter-source spacing of 10 primary beams on the sky, allowing for the varying set of source sizes in a single sky simulation. Between $S_{1.4\ \mathrm{GHz}} = 10$ μJy and 100 nJy the minimum resolution requirement to avoid natural confusion ranges from 0.86″ to 0.07″. Also of interest for deep SKA observations is the natural confusion rate, i.e., the proportion of sources which overlap each other on the plane of the sky. We find that this varies from ~10% of all sources at 10 μJy, rising to ~60% at 100 nJy. This means that at a flux density limit of $S_{1.4\ \mathrm{GHz}} = 100$ nJy, *more than half* of all detected sources will be in line-of-sight coincidence with another source.

Table 2 shows the source distributions by redshifts: here we see that both the FRI and FRII populations extend to very high redshift ($z \sim 8$) at $S_{1.4\ \mathrm{GHz}}$ <10 μJy. These sources would provide the foreground sources to HI line-of-sight experiments (Kanekar and Briggs, 2004; Carilli et al., 2002).

4. SKA specification for AGN continuum survey science

Based on the SKA sky predictions presented here, if the source count continues unchanged down to 100 nJy, there will be about 40 radio sources per square arcmin. We have modelled these sources with finite extents, such that these faint radio sources have dimensions comparable with those of the optical discs of galaxies. At the full sensitivity of the SKA, individual sources will appear blended at the faintest flux density levels.

Resolutions of at least 0.05″ at 1.4 GHz (i.e., 1000 km baselines) are necessary to separate individual sources with a baseline distribution as specified in the SKA Science Requirements specification Jones (2004). However, to image sources with sufficient detail to determine if the emission comes from the disk, star formation or an AGN will require higher resolutions. It is also critical that the SKA resolution at least matches that of complementary facilities (e.g., JWST) for multi-wavelength studies. Also, detailed follow-up of SKA continuum radio surveys will be necessary for high precision cosmology: Planck and its successor missions will require detailed foreground excision, where radio-detected AGN are contaminants to the CMB signal.

Finally, it is vital that the SKA is capable of making simultaneous wide-band observations. These will be used to monitor the time-variability of radio sources, furthering the study of the mechanisms driving intrinsic as well as external variability, e.g., the intra-day variability (IDV) phenomenon.

References

Blundell, K.M., Rawlings, S., Willott, C.J., 1999. In: van Haarlem, M.P. (Ed.), Perspectives on Radio Astronomy: Science with Large Antenna Arrays. ASTRON (NFRA).
Bock, D.C., Large, M.I., Sadler, E.M., 1999. AJ 117, 1578.
Bridle, A.H., Davis, M.M., Fomalont, E.B., Lequeux, J., 1972. AJ 77, 405.
Boyle, B.J., Shanks, T., Peterson, B.A., 1998. MNRAS 235, 935.
Carilli, C.L., Gnedin, N.Y., Owen, F., 2002. ApJ 575, 145.
Condon, J.J., Cotton, W.D., Greisen, E.W., Yin, Q.F., Perley, G.B., Taylor, G.B., Broderick, J.J., 1998. AJ 115, 1693.
Condon, J.J., Cotton, W.D., Broderick, J.J., 2002. AJ 124, 675.
Dunlop, J.S., Peacock, J.A., 1990. MNRAS 247, 19.
Falcke, H., et al., 2004. New AR, this issue.
Fanaroff, B.L., Riley, J.M., 1972. MNRAS 167, 31.
Fomalont, E.B., Kellermann, K.I., Partridge, R.B., Windhorst, E.A., Richards, E.A., 2002. AJ 123, 2402.
Fomalont, E.B., Bridle, A.H., Davis, M.M., 1974. A&A 36, 273.
Giallongo, E., Menci, N., Poli, F., D'Odorico, S., Fontana, A., 2000. ApJ 530, L73.
Gruppioni, C., Zamorani, G., de Ruiter, H.R., Parma, P., Mignoli, M., Lari, C., 1997. MNRAS 286, 470.
Haarsma, D.B., Partridge, R.B., Windhorst, R.A., Richards, E.A., 2000. ApJ 544, 641.
Jones, D., 2004. SKA Memo 45 available from www.skatelescope.org.
Jackson, C.A., Wall, J.V., 1999. MNRAS 304, 160.
Jarvis, M.J., Rawlings, S., 2004. NewAR, this issue.
Kanekar, N., Briggs, F.H., 2004. NewAR, this issue.
Haehnelt, M.G., Rees, M.J., 1993. MNRAS 263, 168.
Laing, R.A., Riley, J.M., Longair, M.S., 1983. MNRAS 204, 151.
Mitchell, K.J., Condon, J.J., 1985. AJ 90, 1957.
Norris, R.P., Hopkins, A., Sault, R.J., Mitchell, D.A., Ekers, R.D., Ekers, J., Badia, F., Higdon, J., Wieringa, M.H., Boyle, B.J., Williams, R.E., 2001 in: Cristiani, S., Renzini, A., Williams, R.E. (Eds.), Deep Fields, Springer-Verlag series, ESO Astrophysics Symposia.
Prandoni, I., Gregorini, L., Parma, P., de Ruiter, H.R., Vettolani, G., Zanichelli, A., Wieringa, M.H., 2001. A&A 369, 787.
Prandoni, I., Gregorini, L., Parma, P., de Ruiter, H.R., Vettolani, G., Wieringa, M.H., Ekers, R.D., 2000. A&A 365, 392.
Richards, E.A., 2000. ApJ 533, 611.
Sadler, E.M., et al., 2002. MNRAS 329, 227.
Urry, C.M., Padovani, P., 1995. PASP 107, 803.
van der Hulst, J.M., et al., 2004. NewAR, this issue.
Wall, J.V., Cooke, D.J., 1975. MNRAS 171, 9.
White, R.L., Becker, R.H., Helfand, D.J., Gregg, M.D., 1997. ApJ 475, 479.
Wall, J.V., Jackson, C.A., Shaver, P.A., Hook, I.M., Kellermann, K.I., (astro-ph0408122).